ASIAN JOURNAL OF PHARMACEUTICAL AND CLINICAL RESEARCH

INNOVARE ACADEMIC SCIENCES
Knowledge to Innovation

Vol 19, Issue 1, 2026

Online - 2455-3891
Print - 0974-2441

Research Article

DESIGN AND DEVELOPMENT OF ENZALUTAMIDE-ENCAPSULATED POLYCAPROLACTONE NANOPARTICLES FOR PROSTATE CANCER: A BOX–BEHNKEN STATISTICAL APPROACH

SAMEENA BEGUM[1], NIRANJAN PANDA[2], CH. PRAVEENA[1]*

[1]Department of Pharmacy, Chaitanya Deemed to be University, Warangal, Telangana, India. [2]Department of Pharmaceutics, School of Pharmacy, The Neotia University, Sarisa, West Bengal, India.
*Corresponding author: Email: praveenamr18@gmail.com

Received: 19 August 2025, Revised and Accepted: 13 November 2025

ABSTRACT

Objectives: This study presents the design and development of Enzalutamide (EZ)-encapsulated polycaprolactone (PCL) nanoparticles (NPs) for targeted prostate cancer therapy, employing a statistical Box–Behnken design to optimize formulation parameters.

Methods: NPs were prepared through the emulsion solvent evaporation method and evaluated for particle size, entrapment efficiency (EE) %, and zeta potential. In vivo pharmacokinetic and cytotoxicity studies were carried out to ensure the in vivo efficacy of the optimised formulation.

Results: The formulations exhibited particle sizes ranging from 148 nm to 219 nm, EE% between 70% and 92%, and zeta potentials from −13.4 mV to −32.5 mV, indicating good colloidal stability. Transmission electron microscopy confirmed spherical morphology, while Fourier-transform infrared spectroscopy (FTIR) revealed no significant chemical interactions between EZ and PCL, confirming compatibility. Cytotoxicity studies demonstrated enhanced anticancer activity of the optimized NPs, with a lower half-maximal inhibitory concentration (14.27 µg/mL) value compared to pure EZ (22.24 µg/mL), suggesting improved cellular uptake and therapeutic efficacy. In the pharmacokinetic evaluation, EZ-loaded optimized NPs (Opt-EZ-PCL-NPs) exhibited a threefold enhancement in area under the curve (34.42 µg.h/mL) ($p<0.05$) relative to the pure EZ suspension formulation (11.30 µg.h/mL) ($p<0.05$), reflecting improved systemic bioavailability.

Conclusion: These findings support the potential of PCL-based nanocarriers as an effective delivery system for EZ in PC treatment.

Key words: Enzalutamide, Polycaprolactone, Half-maximal inhibitory concentration, Prostate cancer, Transmission electron microscopy, Box–Behnken design

 DOI: http://dx.doi.org/10.22159/ajpcr.2026v19i1.56565. Journal homepage: https://innovareacademics.in/journals/index.php/ajpcr

INTRODUCTION

Prostate cancer (PC) is the most frequently diagnosed malignancy among men and remains a major cause of cancer-related mortality worldwide. In 2021, the American Cancer Society reported approximately 248,530 new cases and 34,130 deaths due to PC in the United States alone [1]. The incidence is particularly high among men aged 65 years and older, with Black men exhibiting a 60% greater risk and more advanced disease stages compared to Caucasian men [2]. Conventional treatment modalities – including surgery, radiotherapy, and hormonal therapy – are often accompanied by significant adverse effects such as fatigue, immunosuppression, and increased vulnerability to infections, which impair patients' quality of life and treatment adherence [3].

Enzalutamide (EZ), a potent androgen receptor signaling inhibitor, has emerged as a key therapeutic agent for advanced and metastatic PC. It has demonstrated substantial clinical efficacy and a favorable long-term safety profile across multiple pivotal trials [4]. However, EZ presents several formulation challenges, including poor aqueous solubility, low bioavailability, and dose-dependent systemic toxicity, which limit its therapeutic index and necessitate high oral doses to achieve clinical efficacy [5]. These limitations have prompted efforts to develop alternative delivery systems that can enhance drug solubility, prolong circulation time, and enable targeted release.

Previous studies have explored various EZ-based formulations, including solid dispersions, lipid nanoparticles (NPs), and polymeric micelles, aiming to improve pharmacokinetics and reduce systemic exposure [6]. While these approaches have shown promise, they often lack scalability, exhibit limited control over release kinetics, or fail to achieve optimal encapsulation efficiency. Moreover, few studies have applied robust statistical modeling to systematically optimize formulation parameters for EZ delivery.

Nanotechnology offers a transformative platform for cancer therapeutics, enabling precise drug delivery and improved therapeutic outcomes through engineered NPs [7]. Polycaprolactone (PCL), a biodegradable and biocompatible polymer, has gained attention for its ability to encapsulate hydrophobic drugs and provide sustained release without requiring surgical removal [8]. PCL-based NPs (PCL-NPs) have previously been used to deliver chemotherapeutics such as cisplatin, demonstrating favorable physicochemical properties and anticancer efficacy [9,10].

The present study introduces a novel approach for the design and development of EZ-PCL-NPs using a Box–Behnken design (BBD). This work is distinguished by its integration of EZ into a biodegradable polymeric matrix to overcome solubility and toxicity limitations, and by the application of response surface methodology (RSM) to optimize key formulation variables such as polymer concentration, drug loading, and surfactant levels. The NPs are further characterized using Fourier-transform infrared spectroscopy (FTIR) and transmission electron microscopy (TEM) to confirm drug–polymer interactions and nanoscale morphology. This statistically guided, scalable formulation strategy represents a significant advancement in EZ delivery and offers potential clinical relevance in PC management.

METHODS

Materials

EZ and PCL were purchased from AET Labs, Hyderabad. Polyvinyl alcohol (PVA), dichloromethane, Distilled Water, phosphate buffer

saline (PBS), Sodium Hydroxide, and Potassium Dihydrogen Phosphate; all of these chemicals were purchased from SD Fine Chemicals.

Preparation of EZ-PCL-NPs

EZ-PCL-NPs are commonly prepared by the emulsion solvent evaporation method, where PCL is first dissolved in distilled water at a controlled pH and stirred until fully solubilized [11]. Then stir the solution until both the PCL and EZ are completely dissolved. After that, a desolvating agent such as ethanol is then slowly introduced to induce the formation of NPs through protein precipitation. To stabilize all these particles, a crosslinking agent like PVA is added [12]. The resulting NPs are purified by centrifugation for 20–30 min and are washed to remove free drug and residual chemicals, followed by lyophilization for storage. Then, the NPs are again resuspended in a cryoprotectant solution, such as Mannitol. The final formulation is characterized by size, drug loading efficiency, surface charge, and drug release behavior, making it a promising delivery system for targeted cancer therapy [13].

Systematic optimization of the EZ-PCL-NPs using experimental design

BBD was employed for response surface optimization of the SLNs. The amount of PCL (mg), PVA (%), and sonication time (min) were taken as the highly influential factors for optimization of the PCL-NPs, which were evaluated for the particle size (nm), entrapment efficiency (EE) (%), and zeta potential as the dependent variables. Design Expert software version 12 (Stat-Ease Inc., MN, U.S.A.) was used for applying BBD, where a total of 17 trial formulations of EZ-PCL-NPs with 5 center points were performed and evaluated for the responses. The mathematical model establishment, data analysis, and statistical validity measurement were performed. Model suitability was confirmed on the basis of p-value, correlation coefficient, and predicted error. The final step of selection of the optimized formulation was carried out by a numerical search method to pass the desirability function. Validation of the mathematical model was carried out by identifying check-point formulations to compare predicted and experimental values of the results, where a percentage prediction error within ±5% was considered acceptable.

Characterization of EZ-PCL-NPs

Particle size, polydispersity index (PDI), and zeta potential

The particle size, PDI, and zeta potential of EZ-PCL-NPs formulations were measured using Zetasizer (Nano ZS, Malvern Instrument, U.K.) at 25°C. The Zetasizer was equipped with a red laser of wavelength λ0=633 nm (He−Ne, 4.0 MW) [14].

EE %

The EE% of the EZ-PCL-NPs formulations was determined by an indirect method where the amount of free drug present in the dispersion was quantified. One milliliter of the prepared EZ-PCL-NPs dispersion was centrifuged at 10,000 rpm for 30 min at 4°C. The supernatant fraction was collected and suitably diluted with buffer. The amount of free drug (unentrapped) in NPs was quantified by ultraviolet (UV) spectroscopy. EE was calculated using the following equation [15,16]

$$EE\ \% = \frac{\text{Amount of drug taken-Amount of unentrapped drug}}{\text{Amount of drug taken}} \times 100$$

Physicochemical characterization of the EZ-PCL-NPs

FTIR spectroscopy

The chemical interactions and structural integrity of EZ within the PCL-NP matrix were evaluated using FTIR spectroscopy. Spectra were recorded using an FTIR spectrometer (PerkinElmer, USA) at ambient temperature (25°C), scanning across the range of 500–4000 cm^{-1}. Samples analyzed included EZ-PCL-NPs, blank PCL NPs, and pure EZ. Characteristic peaks were examined to identify potential shifts, intensity changes, or peak broadening indicative of drug–polymer interactions and successful encapsulation [17].

TEM study

Surface morphology and particle architecture of the EZ-PCL-NPs were assessed using TEM. A drop of NP dispersion was placed onto a carbon-coated copper grid and allowed to air dry. The samples were then visualized under a TEM (JEOL, Japan) operated at an accelerating voltage of 200 kV. TEM imaging provided high-resolution insights into particle shape, size distribution, and surface uniformity, enabling confirmation of nanoscale structure and dispersion quality [18].

In vitro drug release study

The study used the dialysis bag technique to track drug release patterns from EZ-PCL-NPs. The release patterns were examined at a pH of 5.5 to mimic the acidic tumor microenvironment. The dialysis bag (12–14 kDa MWCO, Spectra/ProR4 Dialysis Membrane; Spectrum Laboratories, Inc., Rancho Dominguez, CA) was filled with 1 mg of drug in its free form or a formulation volume equivalent to 1 mg of drug. Dialysis bags were then submerged in 200 mL of acetate buffer, pH 5, containing TritonX-100 (1%), and kept in a shaking water bath (AZZOTA corporation, USA). Drug samples were withdrawn and analyzed at 235 nm using a spectrophotometric technique (Spectro UV-visible double beam, Lab India 3200) [19].

In vitro cell culture studies

Cell culture studies were conducted using PC-3 cell line (human grade IV prostate carcinoma cells) obtained from the National Centre for Cell Science, Pune, India. The lyophilized cells were reconstituted and cultured in tissue culture flasks under standard conditions at 37°C in a humidified incubator maintained with 95% air and 5% CO_2. The cells were routinely cultured in Dulbecco's Modified Eagle's medium supplemented with 10% fetal bovine serum, 100 U/mL penicillin, and 100 µg/mL streptomycin to support optimal growth and proliferation [20].

3-(4,5-dimethylthiazol-2-yl)-2,5-diphenyl tetrazolium bromide (MTT) assay

PC-3 cells (8 × 10^3 cells/well) were seeded into 96-well plates and allowed to adhere for 24 h under standard culture conditions. Following adherence, the cells were treated with blank PCL-NPs, Opt-EZ-PCL-NPs, and a Pure-EZ suspension with concentrations ranging from 0.5 to 50 µg/mL, each prepared in standard culture medium. After 72 h of incubation, the cells were gently washed with PBS and subsequently exposed to MTT solution for 4 h to assess metabolic activity. Post incubation, the cells were washed again with PBS and treated with dimethyl sulfoxide to solubilize the resulting formazan crystals. Absorbance was measured at 570 nm using a microplate reader, with untreated cells serving as the control. Cell viability was calculated as the percentage absorbance of treated groups relative to the control. The half-maximal inhibitory concentration (IC_{50}) values, expressed in µg/mL, were determined for each formulation [21].

Pharmacokinetic study

All the animal investigations were performed as per the requisite protocol approved by the Institutional Animal Ethical Committee of Chaitanya Deemed to be University, Hanamkonda, Telangana, with certificate no (005/2024/1963/PO/RC/S/17). *In vivo* studies were carried out in healthy male Wistar rats of 150–200 g. The animals were housed in individual cages in the animal house for 10 days before the initiation of the study to facilitate environmental acclimatization and had access to feed and water *ad libitum*. 12 h circadian rhythms were maintained, and the temperature was kept constant throughout the study period. The animals were randomly divided into two groups, each comprising six rats. A dose of 2 mg/kg was selected for administration, calculated based on the human-to-rat surface area conversion to ensure appropriate translational relevance. The animals were orally administered with Opt-EZ-PCL-NPs and Pure-EZ suspension. Blood

samples were collected from animals under light anesthesia using a CO2 chamber at specified time intervals of 0.5, 1, 3, 6, 12, 16, 18, and 24 h. Plasma was separated by centrifugation at 10,000 rpm for 15 min. The supernatant liquid was separated and analyzed. The amount of EZ in plasma samples was estimated using HPLC at optimized chromatographic conditions [22].

RESULTS AND DISCUSSION

Optimization

The polynomial equation obtained indicates the effect of the interaction of dependent variables on independent variables. The three levels set for the RSM design for independent and dependent variables are represented in Table 1. A positive value in the equation represents a promising effect, and a negative value represents a disapproving effect.

Table 1: Levels obtained from RSM design for independent variables

Independent variable (X)	Unit	Coded Level		
		Low (−1)	Mid (0)	High (+1)
(X1)	mg	100	150	200
(X2)	%	2	3	4
(X3)	min	2	4	6
Dependent variable (Y)	**Requirement**			
(Y1)	nm	Minimize		
(Y2)	**%**	Maximize		
(Y3)	mV	−25mV–−30mV		

Particle size

Particle size is a critical determinant of the biological performance and stability of polymeric NPs; it governs drug release, cellular uptake, and targeting efficiency in polymeric NPs. Table 2 summarizes the particle sizes of all 17 EZ-PCL-NPs batches, which ranged from 148±11.42 to 219±10.88 nm. The polynomial equation presented in Table 3 reveals that particle size was significantly influenced by the independent variables and their interactions

Particle size(Y1)=182+31.12X1+0.1250X2−2.75X3+1.50X1X2+2.75X1X3 + 1.25X2X3−0.5000$X1^2$+2.00$X2^2$+4.25$X3^2$

Table 3 presents the quadratic model analysis, revealing a statistically significant response with an F-value of 65.63 and a p<0.0001. An increase in PCL concentration (X1) leads to a corresponding rise in NP size, likely due to enhanced polymer availability, increased organic phase viscosity, and reduced diffusion rates during particle formation, which collectively promote the development of larger particle cores. Similar findings were reported by Manning *et al.* in 2023 [23], who observed a comparable increase in NP size with elevated PCL concentrations. The amount of PVA% (X2) affects synergistically on particle size. This is because a higher PVA% content may lead to slower desolvation, promoting the formation of larger particles due to extended growth phases. Kitayama *et al.* reported similar results in 2023 [24]. Prolonged sonication during the synthesis of PCL-NPs results in a marked reduction in particle size, attributed to enhanced cavitation and shear forces that facilitate efficient droplet fragmentation. In contrast, shorter sonication times yield larger particles due to limited energy input, leading to inadequate dispersion and increased droplet coalescence [25] (Fig. 1).

Table 2: BBD for EZ-PCL-NPs with responses

Formulation	X1	X2	X3	Particle size (nm)	EE (%)	Zeta potential (mV)	PDI
EZ-PCL-NP1	100	4	4	148±11.42	71±1.42	−13.4±0.14	0.42±0.04
EZ-PCL-NP2	200	3	2	213±10.46	87±2.45	−32.5±0.21	0.31±0.03
EZ-PCL-NP3	150	3	4	181±12.77	81±1.89	−19.8±0.18	0.41±0.06
EZ-PCL-NP4	200	2	4	216±11.32	91±1.64	−31.5±0.14	0.47±0.02
EZ-PCL-NP5	200	4	4	219±10.88	88±1.67	−30.5±0.12	0.51±0.07
EZ-PCL-NP6	150	3	4	183±11.32	82±2.66	−20.7±0.10	0.43±0.04
EZ-PCL-NP7	100	2	4	151±10.11	75±2.11	−16.5±0.12	0.44±0.02
EZ-PCL-NP8	150	4	6	186±13.41	84±1.98	−21.4±0.14	0.46±0.05
EZ-PCL-NP9	150	3	4	185±12.23	83±1.67	−22.3±0.13	0.40±0.01
EZ-PCL-NP10	150	4	2	191±12.14	82±2.11	−20.7±0.16	0.44±0.02
EZ-PCL-NP11	150	3	4	179±13.47	84±2.47	−21.7±0.14	0.47±0.03
EZ-PCL-NP12	200	3	6	215±10.02	92±3.11	−29.7±0.22	0.47±0.04
EZ-PCL-NP13	100	3	2	162±11.08	77±3.66	−15.6±0.31	0.42±0.05
EZ-PCL-NP14	150	3	4	182±13.01	82±2.99	−21.4±0.22	0.39±0.02
EZ-PCL-NP15	150	2	6	183±10.67	83±4.11	−22.7±0.21	0.42±0.03
EZ-PCL-NP16	150	2	2	193±11.44	81±2.78	−20.6±0.13	0.44±0.02
EZ-PCL-NP17	100	3	6	153±12.33	70±1.65	−16.7±0.12	0.46±0.06

All values are expressed as mean±standard deviation; (n=3). EZ: Enzalutamide, PCL: Polycaprolactone, NP: Nanoparticles

Table 3: Box–Behnken design: Regression coefficients with *P* values and quadratic equation

Parameter	Responses					
	Particle size		EE %		Zeta potential	
	F-value	p-value	F-value	p-value	F-value	p-value
Model	65.63	<0.0001	24.26	<0.0002	50.06	<0.0001
Lack of fit	4.95	0.0782	2.85	0.1689	1.51	0.3417
R^2	0.9883		0.9689		0.9847	
Adjusted R^2	0.9732		0.9290		0.9650	
Predicted R^2	0.8485		0.6459		0.8589	

Quadratic model

Y1=+182+31.12X1+0.1250X2−2.75X3+1.50X1X2+2.75X1X3+1.25X2X3−0.5000$X1^2$+2.00$X2^2$+4.25$X3^2$

Y2=+82.82+8.13X1−0.7500X2+0.2500X3+0.2500X1X2+3.00X1X3+0.0001X2X3−1.41$X1^2$−0.16$X2^2$+0.0900$X3^2$

Y3=−21.18−7.75X1+0.6625X2−0.1375X3−5250X1X2+0.9750X1X3+3500X2X3−2.03$X1^2$+02400$X2^2$−0.4100$X3^2$

EE analysis

The EE% in EZ-PCL-NPs significantly influences drug loading capacity and release kinetics. EE% for the 17 experimental formulations ranged from 70±1.65% to 92±3.11%, as detailed in Table 2. The quadratic model derived from the BBD provided a predictive equation for EE%, incorporating the influence of formulation variables. This equation enables the identification of optimal conditions for achieving high EE and supports the rational design of NP-based drug delivery systems.

$$EE\ (Y2)=82.82+8.13X1-0.7500X2+0.2500X3+0.2500X1X2+3.00X1X3+0.0001X2X3-1.41X1^2-0.16X2^2+0.0900X3^2$$

The quadratic model analysis for EE% presented in Table 3 yielded an F-value of 24.26 and a $p<0.0002$, indicating a statistically significant model fit. The response surface equation revealed that the EE of NPs increases with rising concentrations of PCL (X1), primarily due to the enhanced availability of the polymer matrix to entrap the drug molecules. PVA concentration (X2) demonstrated a positive influence on EE%. This is due to stabilization of the emulsion interface and modulation of external phase viscosity, which collectively minimized drug diffusion into the aqueous phase and enhanced encapsulation within the PCL matrix [26]. Similar results were reported by Anastasia *et al*. (2023). These trends are visually represented in the response surface plot (Fig. 2).

Zeta potential

Zeta potential plays a critical role in determining the stability of NPs. The zeta potential obtained in a range from −13.4±0.14 to −32.5±0.21 mV (Table 2). The quadratic equation for zeta potential is as follows:

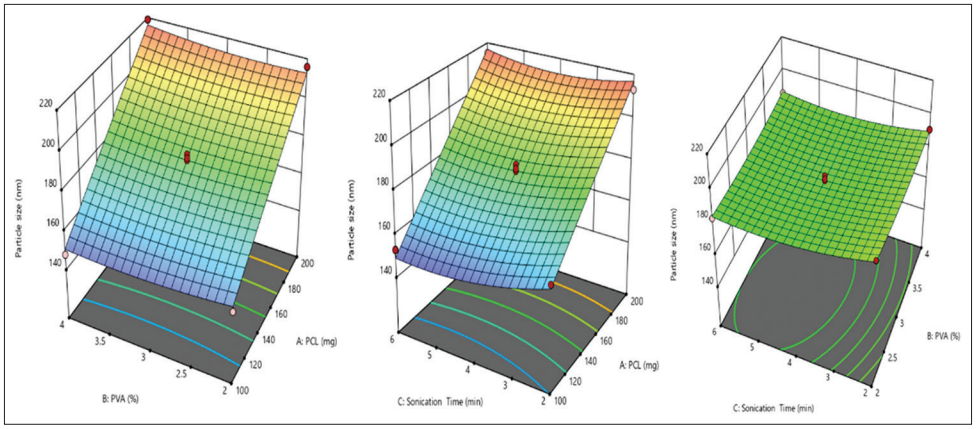

Fig. 1: Effect of the independent variable on particle size

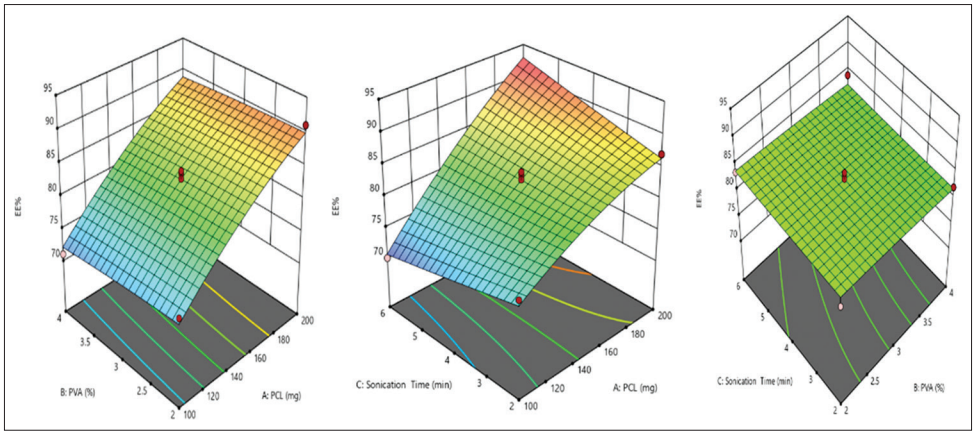

Fig. 2: Effect of independent variable on entrapment efficiency

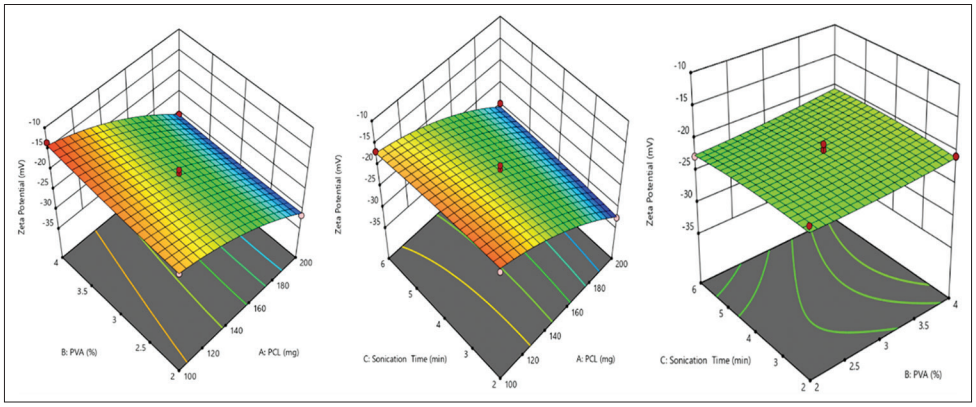

AQ3

Fig. 3: Effect of independent variable on zeta potential

Zeta potential (Y3)=−21.18−7.75X1+0.6625X2−0.1375X3−5250X1X2 +0.9750X1X3+ 3500X2X3−2.03X1^2+02400X2^2−0.4100X3^2

The quadratic model analysis for zeta potential (Table 3) yielded an F-value of 50.06 and a p<0.0001, indicating a statistically significant response. It was observed that increasing the concentration of PCL (X1) in the NP formulation led to a reduction in the magnitude of zeta potential, likely due to the hydrophobic nature of PCL and its limited surface ionization, which diminishes surface charge density and colloidal stability; similar trends have been reported by Kolluru *et al*. in 2020 [26,27]. The effect on zeta potential trends are visually represented in the response surface plot (Fig. 3).

Analysis of PDI

PDI is a key metric used across polymer science, nanotechnology, and drug delivery systems to describe the uniformity of particle or polymer size distribution. The PDI values range from 0.31±0.04 to 0.51±0.07 (Table 2). The concentration and molecular weight of PCL significantly influence the PDI of the resulting NPs. Elevated PCL concentrations tend to increase viscosity during nanoprecipitation, leading to broader particle size distributions and higher PDI values [27].

Optimization and validation of the EZ-PCL-NPs formulation

The Opt-EZ-PCL-NPs formulation was identified by applying constraints to the dependent variables, as outlined in Table 3. Using point prediction analysis in Design Expert Software version 12, the formulation with the highest desirability – approaching a value of 1 – was selected. The predicted optimal process parameters were: PCL concentration (X_1) at 150 mg, PVA concentration (X_2) at 3%, and sonication time (X_3) at 3 min. Corresponding predicted response values included particle size (Y_1) of 182 nm, EE (Y_2) of 82.82%, and zeta potential (Y_3) of –21.18 mV.

The optimized formulation was subsequently prepared and characterized for particle size, EE, and zeta potential. The experimentally obtained values particle size (Y_1) of 186.8 nm, EE (Y_2) of 83.45%, and zeta potential (Y_3) of –21.3 mV were found to be in close agreement with the predicted values generated by the RSM, thereby confirming the reliability and validity of the RSM model [28]. The predicted and observed responses for the optimized formulation are represented in the table 4.

Physicochemical characterization of the optimized NP formulation

TEM study

The morphological characterization of EZ-PCL-NPs, presented in Fig. 4, demonstrates a predominantly spherical geometry with a narrow and uniform particle size distribution. These observed particle sizes (186.8nm) are in close agreement with the measurements obtained through dynamic light scattering (DLS), indicating consistency between imaging and scattering-based analytical techniques. It is important to note that minor variations in particle size between DLS and TEM analyses are expected and can be attributed to methodological differences in sample preparation and measurement principles [29].

Assessment of zeta potential and PDI

Zeta potential serves as a key indicator of NP stability within a dispersion, reflecting the degree of electrostatic repulsion among particles. Higher absolute values of zeta potential suggest stronger repulsive forces, thereby minimizing the likelihood of particle aggregation and promoting colloidal stability. The Opt-EZ-PCL-NPs exhibited a zeta potential of −21.3 mV, indicative of moderate stability. The observed negative surface charge on PCL-NPs is primarily due to the presence of ionizable terminal carboxyl or hydroxyl groups on the polymer chains, which dissociate in aqueous media to generate negatively charged species [30]. In addition, the PDI of the formulation was determined to be 0.446, suggesting a moderately narrow size distribution and acceptable homogeneity among the NPs. This value supports the reproducibility and consistency of the formulation process.

In vitro drug release

The release behavior of EZ from both the Pure-EZ suspension and the Opt-EZ-PCL-NPs is illustrated in Fig. 5. The Pure-EZ suspension exhibited a rapid and nearly complete drug release, with 89.12% released within 4 h and reaching 98.65% by 6 h, indicating immediate availability of the drug in the dissolution medium. This rapid release is characteristic of unencapsulated drug systems and may lead to transient peak plasma concentrations, potentially increasing systemic toxicity and reducing the therapeutic window.

In contrast, the Opt-EZ-PCL-NPs demonstrated a biphasic release pattern, consisting of an initial burst followed by a sustained release phase. Within the first 4 h, approximately 59.68% of EZ was released, which corresponds to the initial burst effect. This phase is likely due to the presence of surface-adsorbed and loosely bound drug, as well as unencapsulated EZ associated with the NP exterior. Following the burst phase, the release rate slowed significantly, with 71.47% released at 6 h, and a gradual increase to 97.25% by 14 h, ultimately reaching 99.17% at 24 h. As a non-ionic surfactant, Triton X-100 enhances solubility by forming micelles that encapsulate hydrophobic drug molecules, thereby maintaining a concentration gradient that drives diffusion from the polymer matrix.

This sustained release phase is attributed to the diffusion of EZ from the polymeric core of the PCL matrix, which provides a controlled and prolonged drug release mechanism. Such a release profile is particularly advantageous for anticancer therapy, where sustained systemic exposure is desired to minimize off-target toxicity and enhance drug accumulation at tumor sites [31]. The initial burst may

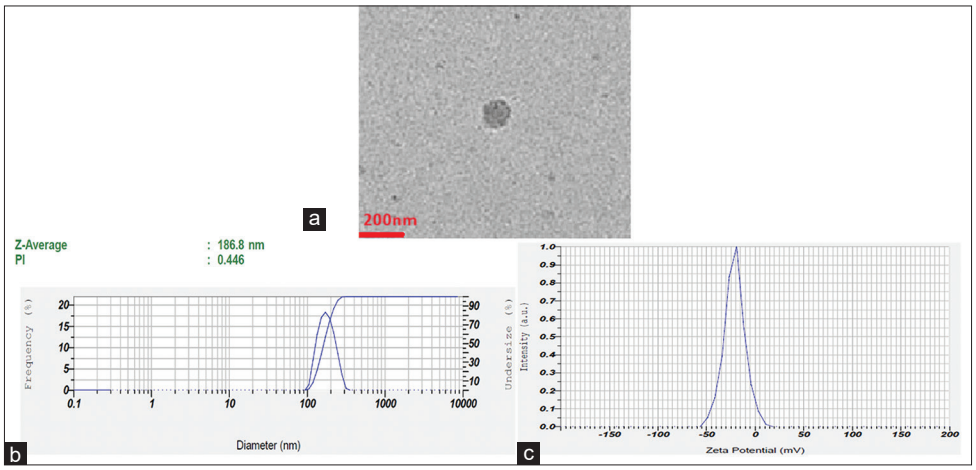

Fig. 4: (a) TEM image, (b) particle size distribution, (c) zeta potential

facilitate rapid therapeutic onset, while the extended release ensures prolonged drug availability, aligning with pharmacokinetic goals for EZ in PC management.

FTIR studies

The FTIR spectra of pure EZ and Opt-EZ-PCL-NPs are shown in Fig. 6, illustrating characteristic functional groups and spectral shifts that confirm successful encapsulation and molecular interactions within the NP matrix. The FTIR spectrum of pure EZ (Fig. 6a) shows characteristic peaks for amide carbonyl (C=O) around 1668.12 cm^{-1}, N–H bending near 1598.26 cm^{-1}, aromatic C=C stretching between 1453.21 cm^{-1}, and C–F stretching around 1236.85 cm^{-1}. In the Opt-EZ-PCL-NPs (Fig. 6b), prominent ester carbonyl peaks of PCL appear near 1726.40 cm^{-1} along with C–O–C stretching vibrations around 1162.12 cm^{-1}, confirming the presence of the polymer. The EZ peaks are retained with reduced intensity, indicating successful encapsulation and possible intermolecular interactions without chemical degradation, suggesting physical entrapment within the polymer matrix [32].

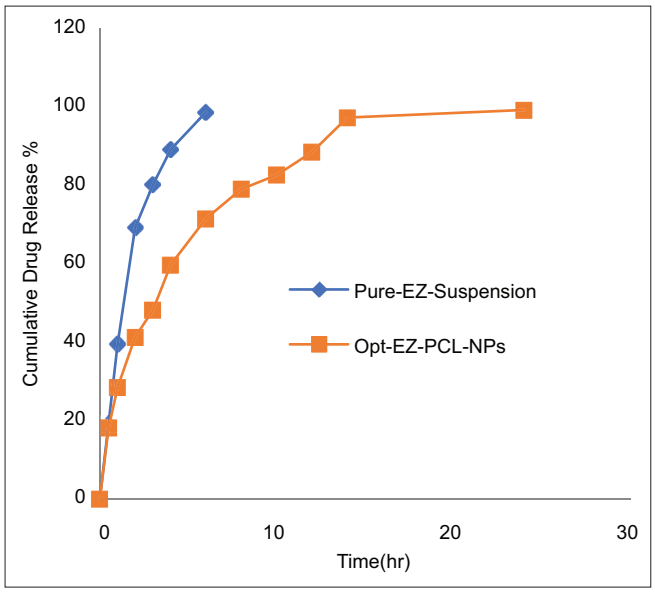

Fig. 5: *In vitro* drug release study

Cytotoxicity studies

The MTT assay results demonstrate a clear dose-dependent reduction in cell viability for both Pure-EZ and Opt-EZ-PCL-NPs when tested against PC-3 cells, while blank PCL-NPs exhibited negligible cytotoxicity across all tested concentrations (0.5–50 µg/mL), maintaining cell viability above 99%, confirming their biocompatibility. Pure EZ showed moderate cytotoxicity, with cell viability decreasing from 95.11% at 0.5 µg/mL to 21.32% at 50 µg/mL (Fig. 7). In contrast, Opt-EZ-PCL-NPs exhibited enhanced cytotoxicity, reducing cell viability more effectively – from 92.45% at 0.5 µg/mL to just 9.25% at 50 µg/mL. This improved performance is attributed to sustained drug release, enhanced cellular uptake, and possible synergistic effects of NP-mediated delivery [33]. The calculated IC_{50} values further support this observation, with Opt-EZ-PCL-NPs achieving a lower IC_{50} of 14.27 µg/mL compared to 22.24 µg/mL for Pure-EZ, indicating superior potency of the NP formulation. These findings suggest that encapsulation of EZ within PCL-NPs significantly enhances its anticancer efficacy against androgen-independent PC cells.

In vivo pharmacokinetic studies

The comparative pharmacokinetic analysis between Pure EZ Suspension and Opt-EZ-PCL-NPs clearly demonstrates the superior performance of the NP-based formulation in enhancing systemic drug exposure and prolonging therapeutic retention (Fig. 8). Following oral administration, Opt-EZ-PCL-NPs achieved a markedly higher Cmax of 4.91 µg/mL compared to 1.56 µg/mL for the Pure EZ Suspension, indicating improved absorption and bioavailability. This enhancement is further substantiated by the area under the curve (AUC) values, where Opt-EZ-PCL-NPs exhibited a three-fold increase (34.42 µg.h/mL) over the suspension (11.30 µg.h/mL), reflecting sustained systemic exposure and efficient drug utilization. The AUMC values (220.41 vs. 62.67 µg·h^2/mL) reinforce the extended residence time of EZ in systemic circulation when delivered through PCL-NPs. This prolonged exposure is attributed to the controlled release kinetics and protective encapsulation offered by the polymeric matrix, which likely mitigates premature metabolism and clearance [34,35].

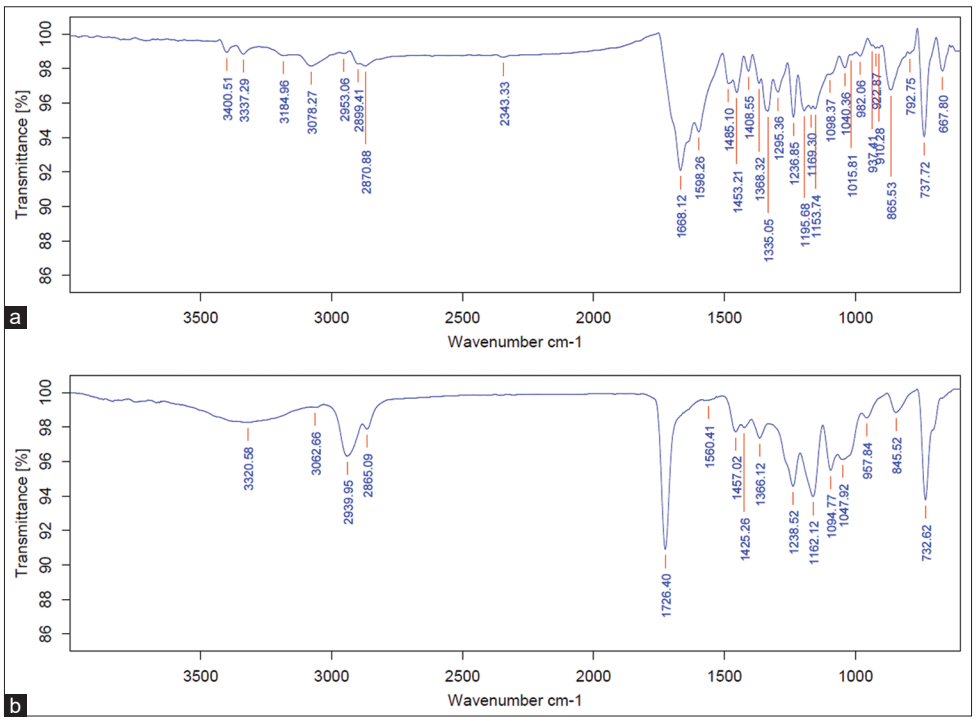

Fig. 6: (a) FTIR of pure enzalutamide, (b) FTIR of optimized formulation. FTIR: Fourier-transform infrared spectroscopy

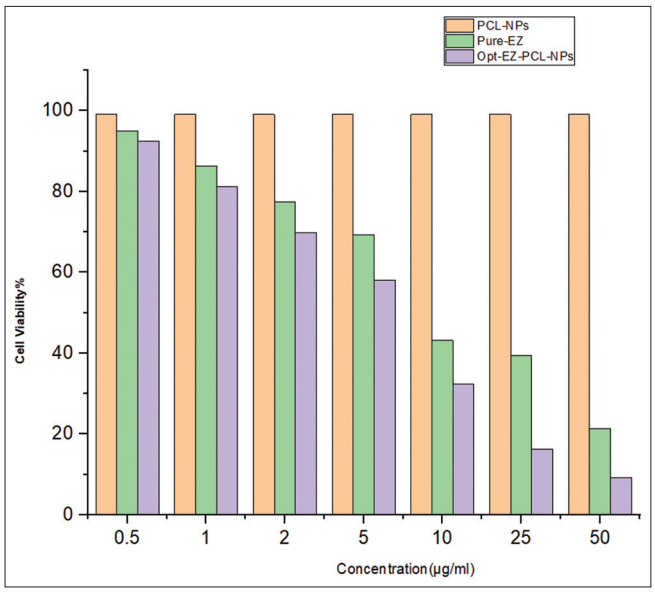

Fig. 7: Cytotoxic study

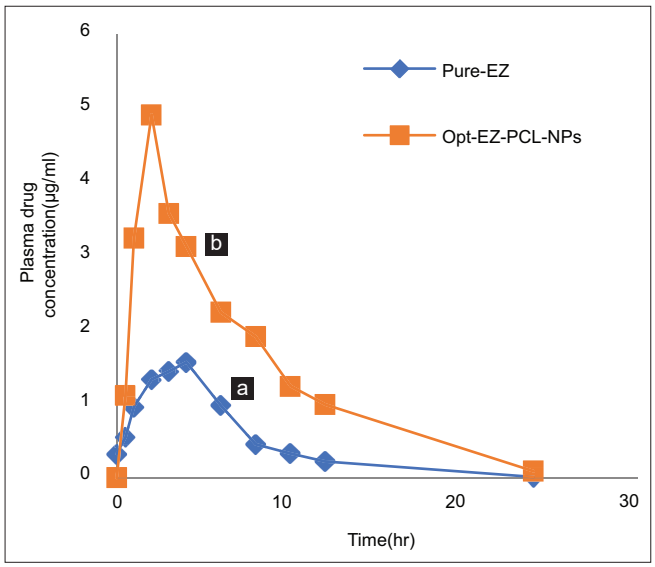

Fig. 8: Plasma concentration time profiles of EZ in Wistar rats: (a) Pure EZ suspension, (b) Opt-EZ-PCL-NPs. EZ: Enzalutamide

Table 4: Predicted and observed responses for optimized formulation

Responses	Predicted	Observed	% of error
Particle size (nm)	182nm	186.8	2.6
Entrapment efficiency (%)	82.82	83.45	0.76
Zeta potential (mV)	−21.18	−21.3	0.56

Moreover, the elimination rate constant (Ke) for Opt-EZ-PCL-NPs (0.047 h^{-1}) was significantly lower than that of the suspension (0.085 h^{-1}), resulting in an extended half-life (t½) of 14.5 h versus 8.13 h. This suggests a slower elimination profile, which is advantageous for maintaining therapeutic plasma levels over time.

The mean residence time (MRT) also improved modestly with the NP formulation (6.40 h vs. 5.54 h), indicating a more sustained pharmacokinetic behavior. While the MRT increase is less pronounced than other parameters, it complements the overall trend of prolonged drug retention and controlled release. The pharmacokinetic parameters of EZ after oral administration of Pure-EZ Suspension and Opt-EZ-PCL-NPs dispersion at a dose of 2 mg/kg are presented in the table 5.

Table 5: Pharmacokinetic parameters of EZ after oral administration of Pure-EZ Suspension and Opt-EZ-PCL-NPs dispersion at the dose of 2 mg/kg

Parameter	Pure EZ suspension	Opt-EZ-PCL-NPs
C_{max} (µg/mL)	1.56	4.91
Area under the curve	11.30	34.42
AUMC(µg/mL.h^2)	62.67	220.41
K_e (h^{-1})	0.085	0.047
$t_{1/2}$ (h)	8.13	14.5
Mean residence time (h)	5.54	6.40

EZ: Enzalutamide, PCL: Polycaprolactone, NP: Nanoparticles

In summary, both the quantitative data and graphical trends underline the superior pharmacokinetic profile of Opt-EZ-PCL-NPs. The NP formulations offer enhanced bioavailability, prolonged systemic retention, and controlled drug release, making them promising candidates for oral delivery of EZ. These improvements could translate into reduced dosing frequency, improved patient compliance, and enhanced therapeutic outcomes.

CONCLUSION

EZ, a potent androgen receptor inhibitor used in PC therapy, suffers from poor aqueous solubility and limited bioavailability, which restricts its therapeutic efficacy and leads to systemic side effects such as immune suppression and off-target toxicity. To overcome these limitations, EZ was successfully encapsulated into PCL NPs using the solvent evaporation method – a widely adopted technique for formulating hydrophobic drugs due to its simplicity, scalability, and ability to produce uniform nanosized particles. The Opt-EZ-PCL-NPs demonstrated a particle size below 200 nm, confirmed through DLS, zeta potential measurements, and TEM. The spherical morphology and narrow size distribution are critical for passive tumor targeting through the enhanced permeability and retention effect, facilitating better accumulation in cancerous tissues. The FTIR revealed a transition of EZ from its crystalline to amorphous state upon encapsulation, along with no significant chemical interactions between the drug and polymer – indicating successful entrapment and compatibility. This amorphization is known to enhance dissolution rates and bioavailability of poorly soluble drugs. Cytotoxicity studies against cancer cells showed that Opt-EZ-PCL-NPs exhibited superior anticancer activity compared to pure EZ, likely due to improved cellular uptake and sustained drug release. *In vitro* and *in vivo* pharmacokinetic evaluations further confirmed prolonged drug release for up to 24 h and significantly enhanced bioavailability, validating the potential of PCL-NPs as an efficient drug delivery system. The Opt-EZ-PCL-NPs demonstrated a threefold increase in AUC (34.42 µg.h/mL) compared to the pure EZ suspension (11.30 µg.h/mL), indicating significantly enhanced systemic bioavailability.

Overall, the developed PCL-based nanocarrier system addresses the major challenges associated with conventional EZ formulations by improving solubility, enhancing tumor penetration, and reducing systemic toxicity – offering a promising strategy for targeted and effective PC therapy.

ACKNOWLEDGMENTS

Authors are thankful to the Institutional Animal Ethical Committee of Chaitanya Deemed University, Hanamkonda, Telangana, for providing facilities to carry out the animal investigations as per the requisite protocol approval of said committees. The authors acknowledge the chairman and principal of Anwarul Uloom College of Pharmacy

in Hyderabad, Telangana, for obtaining permission to conduct the research.

AUTHOR CONTRIBUTIONS

Ms. Sameena Begum contributed to Conceptualization, investigation, data curation, and writing the original draft. Dr. Niranjan Panda contributed to writing, review and editing. Dr. Ch. Praveena acted as supervisor.

CONFLICTS OF INTEREST

The author reports no financial or any other conflicts of interest in this paper.

FINANCIAL SUPPORT

There is no funding to report.

REFERENCES

1. Elmehrath AO, Afifi AM, Al-Husseini MJ, Saad AM, Wilson N, Shohdy KS, *et al*. Causes of death among patients with metastatic prostate cancer in the US from 2000 to 2016. JAMA Network Open. 2021 Aug 02;4(8):e2119568.
2. Parida GR, Pattnaik G, Behera A, Sahoo S, Mohanty D. Development optimization of sorafenib-loaded Plga nanoparticles guided by *in silico* computational tools. Int J App Pharm. 2024 Jul 07;16(4):135-41.
3. Shafiekhani M, Shahabinezhad F, Tavakoli Z, Tarakmeh T, Haem E, Sari N, *et al*. Quality of life associated with immunosuppressant treatment adherence in liver transplant recipients: A cross-sectional study. Front Pharmacol. 2023 Feb 24;14:1051350.
4. Armstrong AJ, Azad AA, Iguchi T, Szmulewitz RZ, Petrylak DP, Holzbeierlein J, *et al*. Improved survival with enzalutamide in patients with metastatic hormone-sensitive prostate cancer. J Clin Oncol. 2022 May 20;40(15):1616-22.
5. Podgoršek E, Mehra N, Van Oort IM, Somford DM, Boerrigter E, Van Erp NP. Clinical pharmacokinetics and pharmacodynamics of the next generation androgen receptor inhibitor-darolutamide. Clin Pharmacokinet. 2023 Aug;62(8):1049-61.
6. AlMousa LA, Pandey P, Lakhanpal S, Kyada AK, Nayak PP, Hussain A, *et al*. An updated review deciphering the anticancer potential of pentacyclic triterpene lupeol and its nanoformulations. Front Pharmacol. 2025 May 09;16:1594901.
7. Das KP, Chandra J. Nanoparticles and convergence of artificial intelligence for targeted drug delivery for cancer therapy: Current progress and challenges. Front Med Technol. 2023 Jan 06;4:1067144.
8. Pawar R, Pathan A, Nagaraj S, Kapare H, Giram P, Wavhale R. Polycaprolactone and its derivatives for drug delivery. Polym Adv Technol. 2023 Oct;34(10):3296-316.
9. Mahmoud BS, McConville C. Development and optimization of irinotecan-loaded PCL nanoparticles and their cytotoxicity against primary high-grade glioma cells. Pharmaceutics. 2021 Apr 13;13(4):541.
10. Chowdhury R, Sharma HK. Prostate cancer: Current and new drug delivery systems. In: Drug Delivery Landscape in Cancer Research. United States: Academic Press; 2025 Jan 01. p. 351-73.
11. Ahmadi H, Haddadi-Asl V. Curcumin-loaded polycaprolactone nanoparticles prepared by emulsion evaporation stabilized with a pH-responsive emulsifier. Polym Eng Sci. 2025 Apr 11;65:3147-62.
12. Song B, Cho CW. Applying polyvinyl alcohol to the preparation of various nanoparticles. J Pharm Invest. 2024 May;54(3):249-66.
13. Herdiana Y, Wathoni N, Shamsuddin S, Joni IM, Muchtaridi M. Chitosan-based nanoparticles of targeted drug delivery system in breast cancer treatment. Polymers (Basel). 2021 May 24;13(11):1717.
14. Mohanty DL, Divya N, Zafar A, Warsi MH, Parida GR, Padhi P, *et al*. Development of etoricoxib-loaded mesoporous silica nanoparticles laden gel as vehicle for transdermal delivery: Optimization, *ex vivo* permeation, histopathology, and *in vivo* anti-inflammatory study. Drug Dev Ind Pharm. 2025 May 04;51(5):506-21.
15. Mohanty D, Gilani SJ, Zafar A, Imam SS, Kumar LA, Ahmed MM, *et al*. Formulation and optimization of alogliptin-loaded polymeric nanoparticles: *In vitro* to *in vivo* assessment. Molecules. 2022 Jul 13;27(14):4470.
16. Panda N, Panda KC, Reddy AV, Reddy GV. Process optimization, formulation and evaluation of hydrogel {guargum-g-poly (acrylamide)} based doxofylline microbeads. Asian J Pharm Clin Res. 2014;7(3):60-5.
17. Chroni A, Mavromoustakos T, Pispas S. Curcumin-loaded PnBA- b-POEGA nanoformulations: A study of drug-polymer interactions and release behavior. Int J Mol Sci. 2023 Feb 27;24(5):4621.
18. Alik KL, Pattnaik G, Satapathy BS, Mohanty D, Prasanth PA, Dey S, *et al*. Preparation and optimization of gemcitabine loaded PLGA nanoparticle using Box-Behnken Design for targeting to brain: *In vitro* characterization, cytotoxicity and apoptosis study. Curr Nanomater. 2024 Dec 01;9(4):324-38.
19. Aly GA, Sabra SA, Haroun M, Helmy MW, Moussa N. Bovine serum albumin nanoparticles encapsulating Dasatinib and Celecoxib for oral cancer: Preparation, characterization, and *in-vitro* evaluation. Naunyn Schmiedebergs Arch Pharmacol. 2025 Feb 12;398:9291-306.
20. Ali R, Huwaizi S, Alhallaj A, Al Subait A, Barhoumi T, Al Zahrani H, *et al*. New born calf serum can induce spheroid formation in breast cancer KAIMRC1 cell line. Front Mol Biosci. 2021 Dec 24;8:769030.
21. Sánchez-Díez M, Romero-Jiménez P, Alegría-Aravena N, Gavira-O'Neill CE, Vicente-García E, Quiroz-Troncoso J, *et al*. Assessment of cell viability in drug therapy: IC50 and other new time-independent indices for evaluating chemotherapy efficacy. Pharmaceutics. 2025 Feb 13;17(2):247.
22. Mohanty D, Alsaidan OA, Zafar A, Dodle T, Gupta JK, Yasir M, *et al*. Development of atomoxetine-loaded NLC *in situ* gel for nose-to-brain delivery: Optimization, *in vitro*, and preclinical evaluation. Pharmaceutics. 2023 Jul 20;15(7):1985.
23. Manning AN, Rowlands CE, Saindon H, Givens BE. Tuning the emulsion properties influences the size of poly(caprolactone) particles for drug delivery applications. AAPS J. 2023 Oct 27;25(6):100.
24. Kitayama Y, Takigawa S, Harada A. Effect of poly(vinyl alcohol) concentration and chain length on polymer nanogel formation in aqueous dispersion polymerization. Molecules. 2023 Apr 15;28(8):3493.
25. Ishak KA, Annuar MS, Aris MH. Chain scission by ultrasonication of polycaprolactone with different initial molecular weight and concentration. J Polym Res. 2022 Apr;29(4):134.
26. Anastasia DS, Desnita R, Kurniawan US. Optimization of PVA concentration in the preparation of amlodipine besylate microparticles with ethyl cellulose polymer based on entrapment efficiency. J Pharm Sci Res. 2023 Feb 01;15(2):1033-5.
27. Kolluru LP, Chandran T, Shastri PN, Rizvi SA, D'Souza MJ. Development and evaluation of polycaprolactone based docetaxel nanoparticle formulation for targeted breast cancer therapy. J Nanopart Research. 2020 Dec;22(12):372.
28. Mohammadi A, Nemati S, Mosaferi M, Abdollahnejhad A, Almasian M, Sheikhmohammadi A. Predicting the capability of carboxymethyl cellulose-stabilized iron nanoparticles for the remediation of arsenite from water using the response surface methodology (RSM) model: Modeling and optimization. J Contam Hydrol. 2017 Aug 01;203:85-92.
29. Filippov SK, Khusnutdinov R, Murmiliuk A, Inam W, Zakharova LY, Zhang H, *et al*. Dynamic light scattering and transmission electron microscopy in drug delivery: A roadmap for correct characterization of nanoparticles and interpretation of results. Mater Horiz. 2023;10(12):5354-70.
30. Fan H, Jin Z. Hierarchical porous polycaprolactone microspheres generated via a simple pathway combining nanoprecipitation and hydrolysis. Chem Commun. 2015;51(82):15114-7.
31. Manzari MT, Shamay Y, Kiguchi H, Rosen N, Scaltriti M, Heller DA. Targeted drug delivery strategies for precision medicines. Nat Rev Mater. 2021 Apr;6(4):351-70.
32. Volkova TV, Drozd KV, Surov AO. Effect of polymers and cyclodextrins on solubility, permeability and distribution of enzalutamide and apalutamide antiandrogens. J Mol Liq. 2021 Jan 15;322:114937.
33. Li X, Peng X, Zoulikha M, Boafo GF, Magar KT, Ju Y, *et al*. Multifunctional nanoparticle-mediated combining therapy for human diseases. Signal Transduct Target Ther. 2024 Jan 01;9(1):1.
34. Abasian P, Shakibi S, Maniati MS, Nouri Khorasani S, Khalili S. Targeted delivery, drug release strategies, and toxicity study of polymeric drug nanocarriers. Polym Adv Technol. 2021 Mar;32(3):931-44.
35. Panda N, Reddy AV, Reddy GV, Panda KC. Effect of different grades of HPMC and Eudragit on drug release profile of Doxofylline sustained release matrix tablets and IVIVC studies. Int Res J Pharm. 2015;6(8):493-504.